Analysis of prognostic risk factors and development of a predictive model for fetuses with right aortic arch with mirror-image branching: a prognostic evaluation method based on ultrasound parameter features

Chuan-Min Wei#^, Bin Ma#, Tian-Gang Li^, Gang Wang, Yan-Yan Chen, Pei-Long Li

Department of Ultrasound Diagnosis, Gansu Provincial Maternity and Child-care Hospital, Lanzhou, China

Contributions: (I) Conception and design: CM Wei; (II) Administrative support: TG Li; (III) Provision of study materials or patients: TG Li, B Ma; (IV) Collection and assembly of data: All authors; (V) Data analysis and interpretation: CM Wei; (VI) Manuscript writing: All authors; (VII) Final approval of manuscript: All authors.

#These authors contributed equally to this work and should be considered as co-first authors.

Correspondence to: Tian-Gang Li, MD, PhD. Department of Ultrasound Diagnosis, Gansu Provincial Maternity and Child-care Hospital, No. 143 Qilihe North Street, Qilihe District, Lanzhou 730050, China. Email: litiangang1981@126.com.

Background: Prenatal ultrasound plays a crucial role in the diagnosis and classification of right aortic arch (AO) with mirror-image branching (RAA-MB). The recent research in this area has primarily focused on qualitative diagnosis, neglecting the quantitative analysis of ultrasound factors that impact RAA-MB outcomes. This study used echocardiography to measure prenatal ultrasound parameters for vascular ring and trachea in fetuses with RAA-MB, employing a nomogram model to evaluate factors influencing their prognosis, thereby providing a comprehensive characterization of potential outcomes.

Methods: A retrospective case-control study was conducted from March 2019 to March 2023. A systematic gathering of prenatal echocardiograms and clinical data was completed for a cohort comprising 92 cases of fetal RAA-MB at the Ultrasound Medicine Center of Gansu Provincial Maternity and Child Care Hospital. Participant recruitment was executed through random selection from among those receiving outpatient medical care. Within the cohort, 42 cases were categorized as fetuses with isolated RAA-MB, while the remaining 50 cases were characterized as fetuses with RAA-MB and associated anomalies. Measurements were taken of the angle between the right AO and the ductus arteriosus (DA) (AO-DA), the distance between the AO and DA, the diameter of AO and DA, and the distance growth rate (DGR) of the AO-DA distance. Additionally, measurements were taken of the tracheal anterior-posterior diameter, tracheal left-right diameter, and tracheal circumference in the three-vessel tracheal view. In the AO view, measurements were taken of the tracheal cross-sectional area (TA) and the vessel ring cross-sectional area (VRA). The relationship between these parameters and the prognosis of fetuses with RAA-MB was assessed using logistic regression analysis. A receiver operating characteristic (ROC) curve was constructed to evaluate the diagnostic performance of the predictive model based on these factors.

Results: The multivariate logistic regression analysis revealed that the independent predictive factors for the prognosis of fetuses with RAA-MB were the AO-DA distance [odds ratio (OR) =0.012], TA (OR =0.401), and VRA (OR =1.103) (all P values <0.001). The area under the ROC curve was 0.891 [95% confidence interval (CI): 0.789–0.914; P<0.001], indicating a high accuracy of the model's predictions.

^ ORCID: Chuan-Min Wei, 0009-0003-4665-769X; Tian-Gang Li, 0000-0003-4384-9701.

Conclusions: The AO-DA distance, TA, and VRA are factors that influence the prognosis of fetuses with RAA-MB. The column chart model constructed based on these parameters can effectively provide a reference for predicting the risk of adverse outcomes in fetuses with RAA-MB.

Keywords: Ultrasound echocardiography; right aortic arch with mirror branch; prognosis analysis; nomogram model

Introduction

The abnormal development of the congenital aortic arch (AO) manifests as right AO with mirror-image branching (RAA-MB). Embryological studies have demonstrated the coexistence of both left and right AOs in the early stages of embryonic development. If the bilateral AO structure persists, this results in the formation of a double AO. However, should the left AO of the double arch model degenerate into the left innominate artery, the mirror image structure of the right AO emerges, which is referred to as RAA-MB. RAA typically takes the form of a U-shaped vascular ring, with a portion of it encircling the trachea and esophagus. The development of the vascular ring and the extent of compression on the trachea and esophagus constitute crucial factors in assessing the prognosis of fetuses with RAA-MB (1). Accurate prenatal assessment is essential for determining the optimal surgical time for clinical treatment in children experiencing postpartum tracheal compression. Although prenatal ultrasound has reached a relatively advanced stage in qualitatively diagnosing fetuses with RAA-MB, there is a paucity of reports on the quantitative analysis of factors influencing the prognosis of fetuses with RAA-MB via prenatal ultrasound (2). The three-vessel tracheal section has demonstrated the ability to diagnose vascular ring, but it fails to reflect the severity of fetal prognosis associated with RAA-MB (3). We thus conducted a comprehensive analysis of prenatal ultrasound images for 92 fetuses with RAA-MB, comparing quantitative measurements of prenatal ultrasound parameters between an isolated RAA-MB group (n=42) and an RAA-MB with malformations group. Additionally, we sought to identify the related prognostic factors and aimed to establish a predictive model for assessing the prognosis of fetuses with RAA-MB. The resulting model holds considerable relevance for prognostic prediction assessments in fetuses with RAA-MB. Analyzing and predicting the prognosis of fetuses with RAA-MB during pregnancy is beneficial for expectant mothers in understanding the in-utero development of the fetus and the prognosis of the disease, as this can help prevent unnecessary concerns among pregnant women, thereby avoiding nonessential pregnancy terminations. Additionally, analyzing the prognosis of fetuses with RAA-MB also provides a certain reference basis for postnatal clinical treatment plans for the infants. We present this article in accordance with the STROBE reporting checklist (available at https://qims.amegroups.com/article/view/10.21037/qims-23-1648/rc).

Methods

Study cohort

This retrospective study was conducted in accordance with the Declaration of Helsinki (as revised in 2013) and was approved by the Ethics Committee of Gansu Provincial Maternity and Child-care Hospital. Before undergoing the examinations, all pregnant women were informed about the accuracy and limitations of ultrasound tests and were required to sign informed consent. The participants also provided their written informed consent to publish data from these cases (including publication of images). Between March 2019 and March 2023, a total of 118 fetuses diagnosed with RAA-MB at the Gansu Provincial Maternity and Child-care Hospital were included in this study. After 26 cases that did not meet the inclusion criteria were excluded, a comprehensive analysis was performed on the prenatal echocardiograms and clinical data of the remaining 92 fetuses with RAA-MB. This cohort comprised 42 cases of isolated fetuses with RAA-MB and 50 cases of fetuses with RAA-MB and associated anomalies. The inclusion were the following: (I) singleton pregnancy; (II) a right-sided AO combined with a left arterial duct, with the left arterial duct being consistently connected to the descending
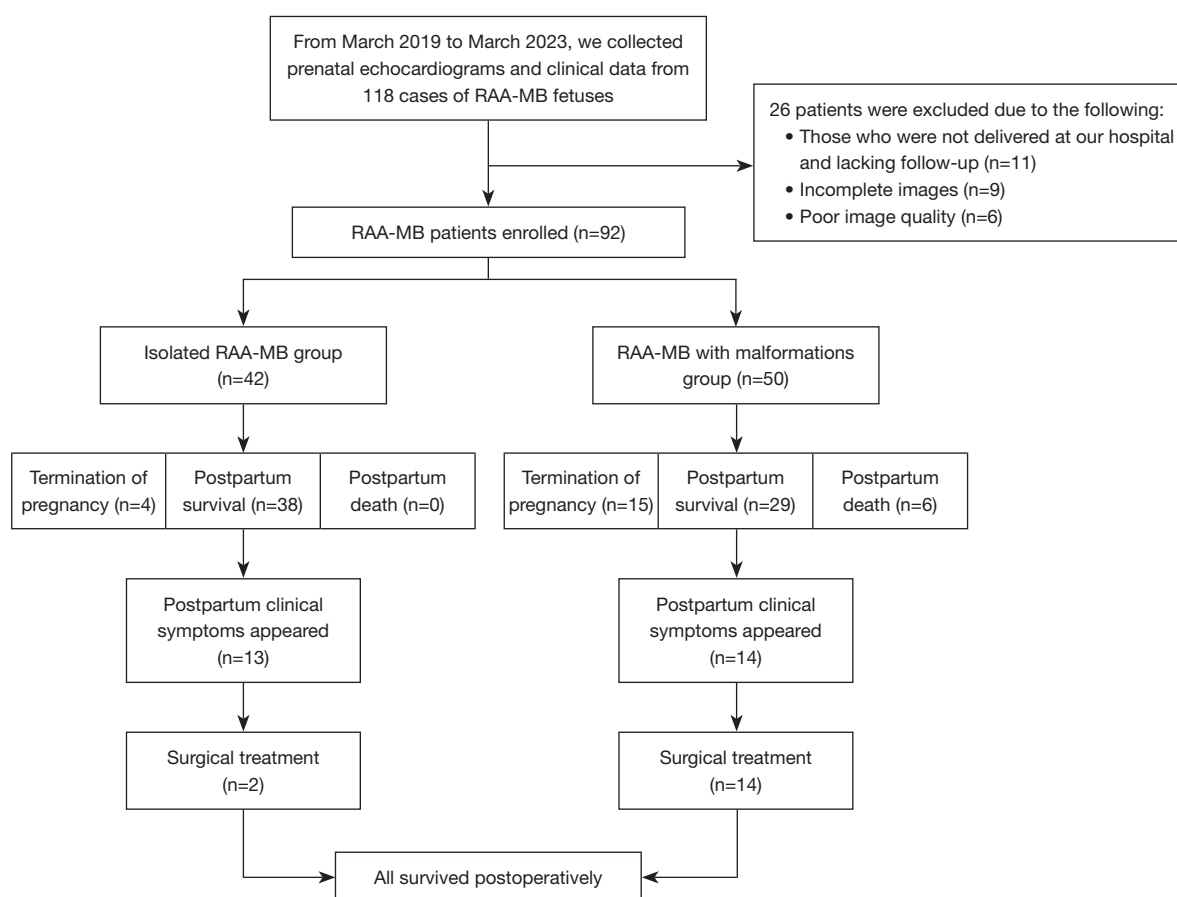
From March 2019 to March 2023, we collected prenatal echocardiograms and clinical data from 118 cases of RAA-MB fetuses

26 patients were excluded due to the following:
• Those who were not delivered at our hospital and lacking follow-up (n=11)
• Incomplete images (n=9)
• Poor image quality (n=6)

RAA-MB patients enrolled (n=92)

Isolated RAA-MB group (n=42)

RAA-MB with malformations group (n=50)

Termination of pregnancy (n=4) | Postpartum survival (n=38) | Postpartum death (n=0)

Termination of pregnancy (n=15) | Postpartum survival (n=29) | Postpartum death (n=6)

Postpartum clinical symptoms appeared (n=13)

Postpartum clinical symptoms appeared (n=14)

Surgical treatment (n=2)

Surgical treatment (n=14)

All survived postoperatively

Figure 1 Flowchart of patient selection. RAA-MB, right aortic arch with mirror-image branching.

aorta (DAO); (III) two-dimensional ultrasound clearly depicting fetal cardiac structures in all planes; (IV) informed consent for the prenatal ultrasound examination of the fetus provided by patients or their family members; and (V) births occurring at Provincial Maternity and Child-care Hospital with mother's consenting to the follow-up of the newborn's postnatal condition. Meanwhile, the exclusion criteria were (I) incomplete clinical or imaging data and (II) births not occurring at Provincial Maternity and Child-care Hospital or lacking follow-up (*Figure 1*).

Instruments and methods

Images were obtained with an eM6C (2.0–5.0 MHz) transducer from a Voluson E10 US system (GE HealthCare, IL, USA). The post-birth follow-up was conducted under the cardiac examination mode of an iE33 color Doppler ultrasonography machine (Philips Healthcare, MD, USA) equipped with a neonatal or pediatric ultrasound probe.

Study procedure

RAA-MB evaluation criteria

RAA-MB was considered to be present when the three-vessel tracheal section of two-dimensional echocardiography and high-definition flow (HD-Flow) color flow diagram showed the AO located on the right side of the trachea, with the arterial duct positioned on the left side and no vagal subclavicular artery present. Moreover, the right AO and left arterial duct needed to form a U-shaped vascular ring surrounding the trachea (*Figure 2A,2B*) and could be clearly visualized in a three-dimensional spatiotemporal image correlation (STIC) blood flow diagram. In RAA-MB, the left arterial duct is connected to the DAO. An anatomical diagram illustrating the blood flow pattern of RAA-MB is presented in *Figure 2C*.

Measurement parameters

The angle between ductus arteriosus (DA) and the (AO-

6872

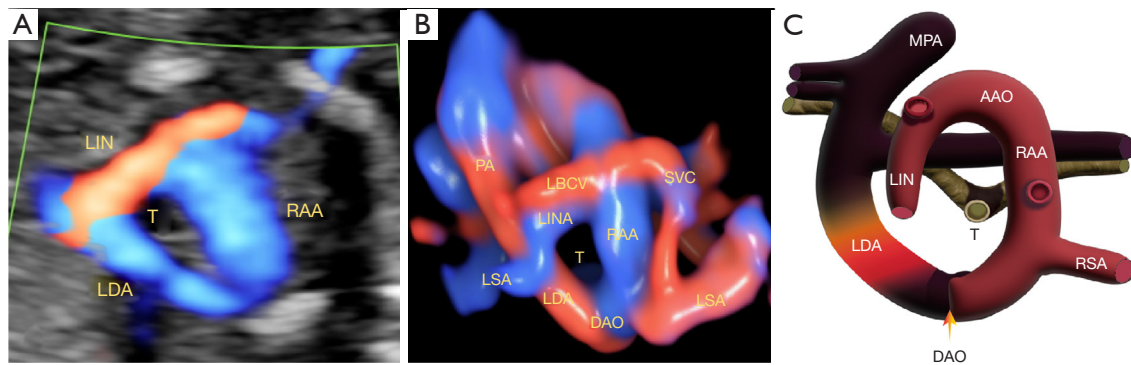**Wei et al. Prognostic analysis study based on ultrasound**

Figure 2 Structural and blood flow schematic of mirror-image right aortic arch across various modes. (A) Mirror image of the right aortic arch prenatal ultrasound and blood flow pattern, with the color flow diagram revealing a U-shaped vascular ring formed by the right aortic arch and ductus arteriosus. (B) The HD-Flow combined STIC displays the three-dimensional spatial connection between the U-shaped vascular ring and the left innominate artery. (C) Image of the anatomic flow pattern of the right aortic arch. LIN, left innominate; RAA, right aortic arch; LDA, left ductus arteriosus; T, trachea; PA, pulmonary artery; LBCV, left brachiocephalic vein; SVC, superior vena cava; LINA, left innominate artery; LSA, left subclavian artery; DAO, descending aorta; MPA, main pulmonary artery; RSA, right subclavian artery; AAO, ascending aorta; HD-Flow, high-definition flow; STIC, spatiotemporal image correlation.

DA angle), distance between the AO and DA (AO-DA distance), inner diameter of the AO, and inner diameter of the DA were assessed. Furthermore, the ratio of inner diameter of the AO to that of the DA and the distance growth rate (DGR) of the AO-DA distance were calculated. Measurements were also obtained for the main tracheal circumference, tracheal cross-sectional area (TA), and the vessel ring cross-sectional area (VRA).

Measurement method

The three-vessel tracheal standard section of the fetus was obtained, and dynamic images were captured for subsequent measurement. Through review of the dynamic image of the three-vessel tracheal section, the end-systolic image was selected as the standard measurement section. Points marking the pulmonary artery, AO, DA, DAO, and trachea were identified on this section. To ensure precision, the ultrasound instrument's screen protractor was activated to accurately outline the standard measurement line.

(I) Measurement of the AO-DA angle: in the three-vessel tracheal view, the AO-DA angle was measured using the angle measurement tool on the screen, which represents the angle between the midline of blood flow in the AO and the DA. The A-line corresponds to the axis connecting the AO, while the P-line corresponds to the axis connecting the ductal arch. The A-line and the extension line of the P-line intersect at point O, resulting in the

measurement of ∠AOP. This AP angle represents the angle between the AO and the DA (*Figure 3A*).

(II) Measurement of the AO-DA distance and the AO and DA diameters: in the three-vessel tracheal view, the midpoint of AO and DA was precisely identified and marked. The diameters of both vessels were measured at the level of the midpoint, and the ratio of the diameter DA to that of the AO diameters was calculated. To ensure consistent and reliable measurement results, the AO-DA distance was determined by measuring the inner boundaries of the AO and DA (*Figure 3B,3C*).

(III) Measurement of the anterior-posterior diameter, left-right diameter, tracheal circumference, and TA. The position of the AO, its branches, pulmonary artery branches, and DA in relation to the trachea were observed. Tracheal compression was assessed in the long-axis view of the trachea (*Figure 4A*), and subsequently, the probe was rotated 90° to obtain a short-axis view in the three-vessel tracheal plane. The trachea was identified, and measurements were obtained after clear visualization of its structure. The two-line perpendicular measurement method was employed to determine the tracheal dimensions, including anterior-posterior diameter and left-right diameter. TA, vascular ring cross-sectional area, and tracheal circumference were measured using manual tracing. Each measurement
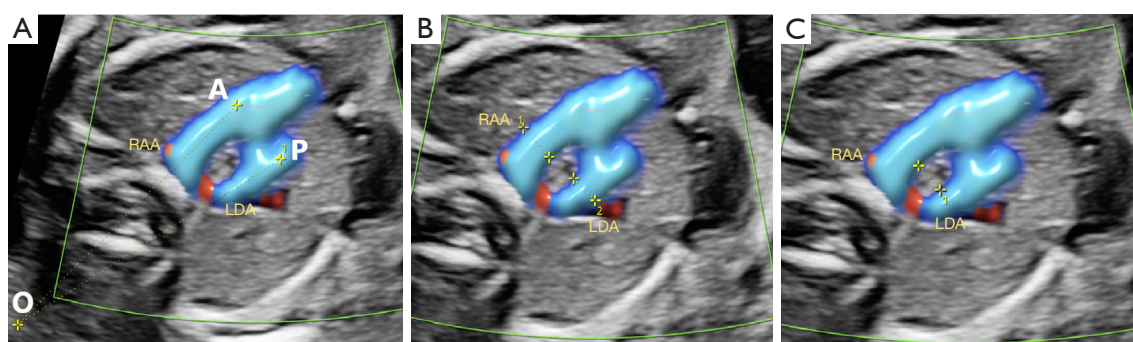
Figure 3 Two-dimensional ultrasound measurement schematic of the mirror branches of the right aortic arch. (A) Measurement schematic of the angle between the right aortic arch (A-line) and left ductus arteriosus (P-line) (AO-DA angle, ∠AOP). (B) Schematic for measuring the inner diameter of the right aortic arch and left ductus arteriosus (AO inside diameter DA inside diameter). (C) Schematic representation of the distance between the right aortic arch and left ductus arteriosus (AO-DA distance). RAA, right aortic arch; LDA, left ductus arteriosus; AO, aortic arch; DA, ductus arteriosus; AO-DA angle, angle between the right aortic arch and the left ductus arteriosus; AO-DA distance, distance between the right aortic arch and left ductus arteriosus.
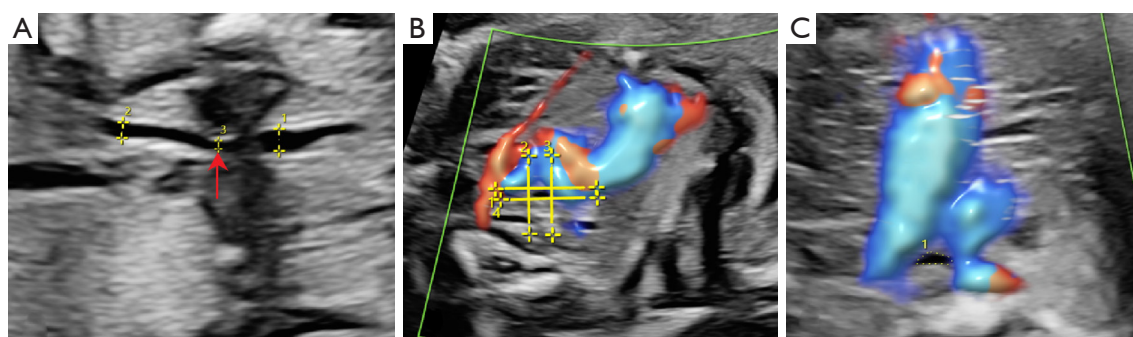

Figure 4 Quantification of tracheal and vascular ring parameters in fetal mirror image right aortic arch across various two-dimensional ultrasound planes. (A) Long-axis view of the trachea for evaluating morphology. The red arrow indicates pronounced tracheal compression leading to segmental narrowing. (B) The two-line perpendicular measurement method for measuring the anterior-posterior diameter and left-right diameter of the trachea. (C) The short-axis view of the trachea for determining the tracheal circumference and cross-sectional area. (Annotation: the numbers 1, 2, 3, etc., in the image hold no specific significance and are merely identification numbers generated during the process of image measurement).

was performed three times, and the average value was calculated (*Figure 4B,4C*).

(IV) Postnatal data collection: data regarding the presence of symptoms related to tracheal or esophageal compression after birth were collected. Follow-up examinations, including ultrasound echocardiography, were conducted on newborns diagnosed prenatally with isolated RAA-MB or RAA-MB with malformations. The follow-up period ranged from 1 month to 3 years after birth, with a focus on monitoring the pregnancy outcome, growth, and development of the cases. Special attention was paid to the occurrence of respiratory symptoms in the newborns after birth, such as wheezing, choking, recurrent respiratory infections, and swallowing difficulties.

Quality control and reproducibility analysis

The fetuses with vascular rings included in this study were evaluated by two experienced physicians, each with more than 10 years of expertise in fetal cardiac ultrasound

diagnosis. These two experienced examiners independently measured different geometric parameters and conducted interrater reliability tests. The measurement results were assessed based on the measurements obtained by both examiners.

Statistical methods

The statistical analysis and construction of the column chart model were performed using SPSS 25.0 (IBM Corp., NY, USA) and R software 4.0.1 (The R Foundation for Statistical Computing). Normally distributed continuous data are presented as the mean ± standard deviation ($\bar{x}$±s), while nonnormally distributed variables were expressed as the median and interquartile range. Chi-square tests were used to analyse categorical data, which are presented as proportions (%). The independent samples t-test was employed for normally distributed continuous variables, while the Mann-Whitney test was used for nonnormally distributed variables. Univariate analysis and multivariate logistic regression analyses were conducted to identify independent risk factors associated with the prognosis of fetuses with RAA-MB and to construct the column chart model. The goodness of fit of the column chart model was assessed using calibration curves. Receiver operating characteristic (ROC) curves were generated, and the area under the curve (AUC) was determined to evaluate the predictive performance of the column chart model for the prognosis of fetuses with RAA-MB. Decision curve analysis (DCA) was used to assess the clinical utility of the model. A two-sided P value <0.05 was considered statistically significant.

Results

In this study, all fetuses exhibited a right-sided AO combined with a left arterial duct, and the left arterial duct was consistently connected to the DAO.

Clinical data and follow-up information of infants with isolated RAA-MB or RAA-MB combined with other anomalies

Among the 50 cases of RAA-MB with associated anomalies, 15 pregnancies were terminated, 29 infants survived after birth, and 6 infants died postnatally for various reasons. These six fetuses were born prematurely due to intrauterine growth restriction and maternal factors, which prevented them from reaching full term. In addition, the fetuses had cardiac structural abnormalities in utero, and postnatally, the infants exhibited clinical symptoms such as pulmonary infection, pulmonary arterial hypertension, and heart failure. After birth, the infants showed weak vital signs, and unfortunately none of them survived. Follow-up within 18 months after birth revealed that out of the 29 surviving infants, 9 experienced respiratory system symptoms, 4 exhibited digestive system symptoms, and 1 had difficulty swallowing. Among these infants, 14 underwent surgical treatment for RAA-MB with associated anomalies. In these 14 cases, the primary objective of surgery for 10 infants was to address additional systemic anomalies, while the remaining 4 infants were premature. Among the premature infants, three underwent surgery due to weakened vital signs resulting from prematurity, and one infant, identified with mild tracheal compression in prenatal ultrasound, experienced recurrent respiratory infections postnatally. Prompt surgical intervention relieved vascular compression, and the postoperative outcomes were favorable. In the subgroup of 42 cases with isolated fetuses with RAA-MB, 4 pregnancies were terminated, and 38 infants survived after birth. During the 1-year postnatal follow-up, eight infants experienced mild respiratory system symptoms, four exhibited digestive system symptoms, and one infant had mild difficulty swallowing. Among the premature infants, two developed respiratory tract infection symptoms postnatally and underwent successful surgical treatment. As of this writing, these infants are in a healthy state (*Table 1*). We conducted a comprehensive statistical analysis on 50 fetuses with RAA-MB, focusing on intracardiac and extracardiac malformations. Our findings revealed that intracardiac malformations occurred at a higher rate than did extracardiac malformations in fetuses afflicted with RAA-MB. Among those with intracardiac malformations, the most frequently observed conditions were atrial septal defects, ventricular septal defects, and tetralogy of Fallot. A higher incidence of hydronephrosis was noted in fetuses with extracardiac malformations (*Table 2*).

Baseline characteristics of patients

A total of 92 patients diagnosed with right AO with RAA-MB were enrolled in this study, including 42 cases of isolated RAA-MB and 50 cases of RAA-MB with associated malformations. The patients were divided into two groups based on the presence or absence of associated malformations: the isolated RAA-MB group (n=42) and the

Table 1 Postnatal follow-up of fetuses with isolated RAA-MB and fetuses with combined anomalies of RAA-MB

Characteristic	Isolated RAA-MB group	RAA-MB with malformations group
Stridor	2 [5]	2 [7]
Respiratory distress	0 [0]	2 [7]
Recurrent respiratory infection	3 [7]	3 [10]
Persistent cough	3 [7]	2 [7]
Dysphagia	1 [2]	1 [3]
Digestive symptoms	4 [10]	4 [13]
Termination of pregnancy	4	15
Postpartum death	0	6
Postpartum survival	38	29

Data are represented as number or number [%]. RAA-MB, right aortic arch with mirror-image branching.

Table 2 Prevalence of congenital malformations in 50 cases of fetal RAA-MB

Combined with malformation	Number of cases	Proportion (%)
Intracardiac malformation		
Simple ventricular septal defect	9	18
Atrial septal defect with ventricular septal defect	13	26
Right ventricular double outlet	6	12
Transposition of the great arteries	3	6
Tetralogy of Fallot	12	24
Right atrial isomerism	4	8
Permanent left upper cavity	3	6
Extracardiac malformation		
Hydronephrosis	7	14
Single umbilical artery	6	12
Right kidney dysplasia	4	8
Cleft lip and palate	5	10
Absence of thymus	2	4
Asplenia syndrome	4	8

RAA-MB, right aortic arch with mirror branch.

RAA-MB with malformations group (n=50). Both groups of fetuses underwent ultrasound examinations during the mid-pregnancy and late-pregnancy periods, and the data from both ultrasound examinations were included in the analysis. The results revealed statistically significant differences in the AO-DA distance, VRA, and TA between the two groups (P< 0.001), indicating that these variables are factors associated with the prognosis of fetuses with RAA-MB (*Table 3*).

Results of univariate and multivariate logistic regression analyses

Univariate and multivariate logistic regression analyses were conducted to preliminarily analyze the ultrasound

6876

Wei et al. Prognostic analysis study based on ultrasound

Table 3 Comparison of baseline characteristics between the RAA-MB group and the RAA-MB group with malformations

Ultrasonic measurement parameter	Isolated RAA-MB group (n=42)				RAA-MB with malformations group (n=50)				t/Z value	P value
	Mid-pregnancy (n=42)	Late pregnancy (n=42)	t/Z value	P value	Mid-pregnancy (n=50)	Late pregnancy (n=50)	t/Z value	P value		
AO-DA distance (mm)	4.25±0.29	5.62±0.85	−9.85[a]	<0.001	3.77±0.37	3.43±0.31	1.52[a]	0.04	11.21[a]	<0.001
AO-DA angle (°)	15.22 (14.08, 15.80)	17.31 (15.84, 18.44)	−5.35[b]	0.01	14.23 (13.15, 15.27)	12.34 (11.17, 14.5)	−1.21[b]	0.02	−5.29[b]	0.01
AO inside diameter (mm)	4.28±0.61	3.97±0.31	2.96[a]	0.004	4.09 (3.89, 4.21)	4.28 (4.28, 4.75)	−7.16[b]	0.00	−2.15[a]	0.03
DA inner diameter (mm)	4.11±0.28	4.68±0.64	−5.26[a]	<0.001	3.73±0.46	4.17±0.33	−5.56[a]	0.00	5.88[a]	<0.001
AO/DA	1.03 (0.94, 1.15)	0.82 (0.75, 0.98)	−4.64[b]	<0.001	1.07 (0.99, 1.16)	1.06 (1.01, 1.14)	−0.08[b]	0.93	−5.56[a]	<0.001
TA distance (mm)	2.45±0.12	2.67±0.22	−5.79[a]	<0.001	2.41±0.14	2.64±0.27	−5.39[a]	0.00	−1.82[b]	0.06
TA left-right diameter (mm)	2.23 (2.12, 2.44)	2.68 (2.55, 2.96)	−6.52[b]	<0.001	2.24 (2.14, 2.47)	2.64 (2.50, 2.93)	−6.50[b]	0.03	−0.29[b]	0.76
TA perimeter (mm)	7.37 (6.98, 7.86)	5.46 (5.13, 5.78)	−5.86[b]	0.005	7.39 (6.95, 7.89)	8.20 (7.82, 8.55)	−5.90[b]	0.00	−0.39[b]	0.69
TA CSA (mm)	4.98 (4.65, 5.30)	5.46 (5.13, 5.78)	−4.37[b]	0.02	4.74 (4.43, 5.15)	5.28 (4.92, 5.64)	−4.92[b]	0.01	−2.39[b]	0.01
VR CSA (mm)	42.96±6.79	51.64±11.22	−4.29[a]	0.01	42.82±6.90	53.06±10.47	−5.77[a]	0.005	−0.14[b]	0.03

Data are presented as mean ± standard deviation or median (interquartile range). [a], statistical analysis performed using chi-square test; [b], statistical analysis performed using Mann-Whitney test. RAA-MB, right aortic arch with mirror branching; AO-DA distance, distance between the right aortic arch and left ductus arteriosus; AO-DA angle, angle between the right aortic arch and the left ductus arteriosus; AO, aortic arch; DA, ductus arteriosus; TA, tracheal anterior; CSA, cross-sectional area; VR, vascular ring.

echocardiographic measurement parameters of the two groups of fetuses. The data from both groups of fetuses with RAA-MB underwent statistical analysis, revealing statistically significant differences between the groups (*Figure 5A-5C*). The parameters that showed statistically significant differences between the two groups, including AO-DA angle, AO-DA distance, TA, and VRA, were included in the regression analyses. The results indicated that the independent factors for predicting the prognosis of fetuses with RAA-MB were AO-DA angle [odds ratio (OR) =0.693], AO-DA distance (OR =0.017), TA (OR =0.517), and VRA (OR =1.036) (all P values <0.001). The univariate logistic regression analysis showed that the AO-DA angle, AO-DA distance, TA, and VRA were individual factors associated with the prognosis of fetuses with RAA-MB, with the AO-DA distance having the highest predictive value for the prognosis of fetuses with RAA-MB and associated anomalies. Further multivariate logistic regression analysis revealed that the independent factors for predicting fetuses with RAA-MB were AO-DA distance (OR =0.012), TA (OR =0.401), and VR (OR =1.103) (all P values <0.001) (*Table 4*).

Construction and validation of the column chart model for predictive factors

The fetal RAA-MB prognostic risk model was validated using a calibration curve based on a multivariate logistic regression model (*Figure 6A-6C*). The calibration curve of the prediction model demonstrated excellent fit with the ideal curve, indicating close agreement between the predicted and actual values and the strong calibration ability of the model. This model holds significant potential for determining clinical benefit. The ROC analysis revealed that the AUC for this model was 0.891 [95% confidence interval (CI): 0.789–0.914; P<0.001], with a sensitivity of 82.5% and a specificity of 76.9% (*Figure 6D*).

Discussion

Congenital vascular ring is a vascular anomaly that occurs during embryonic development and involves the AO, its branches, and the branches of the pulmonary artery. It represents approximately 0.8% to 1.3% of all congenital heart diseases (4). In early embryonic development, if the
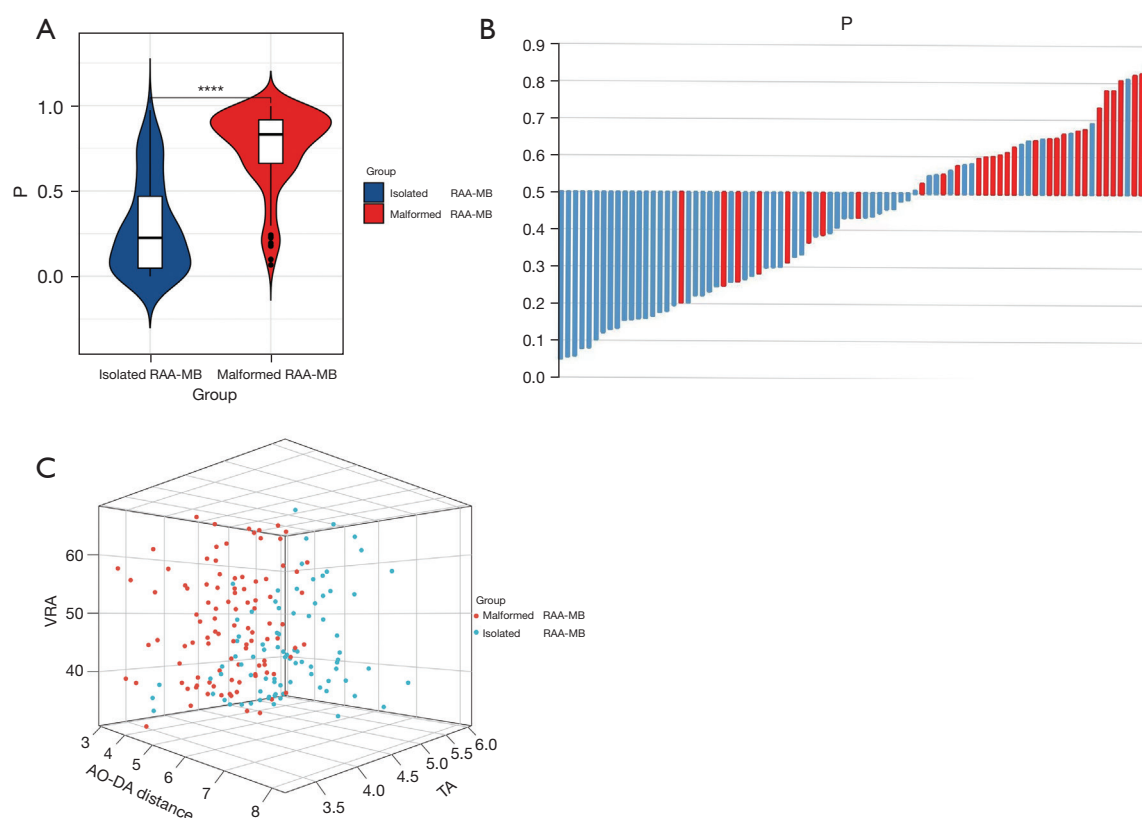
Figure 5 Analysis of prenatal ultrasound measurement parameters in the two groups of fetuses. (A) Comparative analysis reveals a significant statistical difference in the AO-DA distance between the two groups. ****, a statistically significant difference. (B) Examination of the fluctuation process in the AO-DA distance in the two groups. (C) Evaluation of the overall data distribution of AO-DA distance, TA, and VRA in the two groups. RAA-MB, right aortic arch with mirror-image branching; VRA, vessel ring cross-sectional area; AO, aortic arch; DA, ductus arteriosus; TA, tracheal cross-sectional area.

left AO is absorbed while the right AO remains, this results in the formation of a right AO malformation. Right AO can be further classified into two types based on the site of absorption: right AO with aberrant left subclavian artery (RAA-ALSA) and RAA-MB. However, studies indicate that regardless of the position of the ductal arch, RAA will increase the risk of associated heart defects (5,6). RAA-MB typically forms a U-shaped vascular ring and can exist independently or be associated with other cardiac anomalies. RAA-MB itself does not have an impact on cardiovascular physiology and hemodynamics. If RAA-MB is associated with a congenital heart defect, the prognosis is usually determined by the severity of the cardiac defects after birth. In some cases, the vascular ring formed by RAA-MB can potentially exert pressure on the trachea and esophagus, resulting in symptoms including recurrent chronic cough, wheezing, respiratory distress, and swallowing difficulties.

According to the literature, RAA-MB is almost always associated with other congenital cardiac anomalies. Previous research (7) has indicated that fetuses with RAA-MB commonly exhibit concurrent cardiac and extracardiac anomalies, including atrial and ventricular septal defects, tetralogy of Fallot, aortic coarctation, renal pelvis dilation, and cleft lip and palate, in addition to chromosomal abnormalities such as trisomy 13, trisomy 18, and trisomy 21 (8). Consequently, prenatal ultrasound evaluation of fetuses with RAA-MB holds considerable significance in prognostic prediction. This study incorporated prenatal ultrasound measurements of fetuses with RAA-MB and employed quantitative parameters to construct a more visually comprehensible column chart model. The objective was to provide risk assessment for the prognosis of fetuses with RAA-MB and aid clinicians in the early identification of high-risk fetuses with RAA-MB.

6878

Wei et al. Prognostic analysis study based on ultrasound

Table 4 Univariate and multivariate logistic regression results

Characteristic	Single-factor analysis				Multiple-factor analysis			
	Regression coefficient	Standard error	OR (95% CI)	P value	Regression coefficient	Standard error	OR (95% CI)	P value
AO-DA distance	−4.080	0.643	0.017 (0.005–0.060)	<0.001	−4.395	0.734	0.012 (0.003–0.052)	<0.001
AO-DA angle	−0.367	0.084	0.693 (0.588–0.817)	0.01	−0.106	0.175	0.904 (0.689–1.185)	0.54
TA distance	−0.617	0.650	0.539 (0.151–1.930)	0.34	–	–	–	–
TA left-right diameter	−0.039	0.437	0.962 (0.409–2.264)	0.93	–	–	–	–
TA perimeter	−0.112	0.223	0.894 (0.578–1.383)	0.61	–	–	–	–
TA CSA	−0.660	0.293	0.517 (0.291–0.917)	0.02	−0.888	0.459	0.401 (0.157–0.994)	0.04
VR CSA	0.036	0.016	1.036 (1.005–1.069)	0.02	0.098	0.029	1.103 (1.042–1.168)	<0.001

OR, odds ratio; CI, confidence interval; AO-DA angle, angle between the right aortic arch and the left ductus arteriosus; AO-DA distance, distance between the right aortic arch and left ductus arteriosus; TA, tracheal anterior; VR, vascular ring; CSA, cross-sectional area.
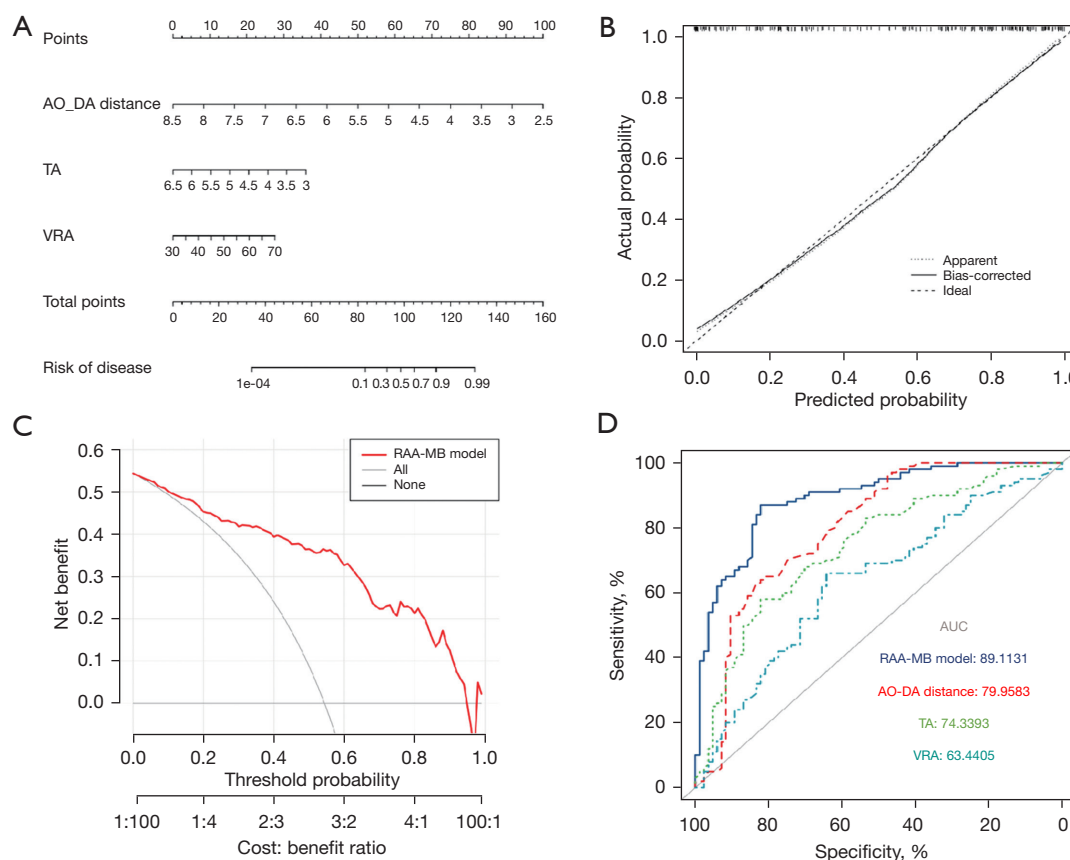

Figure 6 Analysis and validation of a prognostic model based on several features in the nomogram framework. (A,B) The predictive model and calibration curve validation for the prognosis of fetuses with right aortic arch with mirror-image branching. (C,D) A summary comparison of receiver operating characteristic curves for evaluating the predictive performance of the model and individual independent risk factors. AO-DA distance, distance between the right aortic arch and left ductus arteriosus; TA, tracheal cross-sectional area; VRA, vascular ring cross-sectional area; AUC, area under the curve; RAA-MB, right aortic arch with mirror-image branching.

The trachea in fetuses with RAA-MB is situated between the two vessels, creating a space for the trachea. As the vascular ring transitions from a "V" shape to a "U" shape, the AO and DA tend to align parallel to each other, and the bisector of the AO-DA angle also tends to be parallel. A recent study (9) reported that the average AO-DA angle in isolated fetuses with RAA-MB was 22.05°±1.35° and that this angle slightly increased with gestational age. In our study, the findings demonstrated that the average AO-DA angle in fetuses with isolated RAA-MB was 22.14°±1.08°, which aligns with previous research. However, fetuses with RAA-MB and associated anomalies had an average AO-DA angle of 18.73°±2.34°, which was significantly smaller than that of the isolated fetuses with RAA-MB. Furthermore, our study revealed that the average AO-DA distance in isolated fetuses with RAA-MB was 4.86 (range, 4.16–5.74) mm, whereas it was 3.87 (range, 3.27–4.24) mm in fetuses with RAA-MB with associated anomalies, representing a statistically significant difference. We also found that in fetuses with RAA-MB and associated anomalies, the AO-DA distance tended to decrease with an increase in gestational age, but there was no significant correlation with gestational age. Conversely, in isolated fetuses with RAA-MB, the AO-DA distance tended to increase with gestational age, showing a weak but linear positive correlation. This indicates that the AO-DA distance in fetuses with isolated RAA-MB increases to a certain extent as the trachea and surrounding tissue structures grow, following the normal patterns of fetal growth and development. To account for the interference of gestational age, we calculated the DGR. The results revealed that the DGR in the isolated RAA-MB group was significantly higher (approximately twice as high) than that in the RAA-MB with malformations group, which is consistent with our previous analysis, The rate of increase in the AO-DA distance in the RAA-MB with malformations group is relatively slower compared to the isolated RAA-MB group. Compared to isolated RAA-MB, RAA-MB with associated anomalies impedes the development of the AO and DA, suggesting that fetuses with a smaller AO-DA distance in prenatal measurements may have additional anomalies and a poorer prognosis (10). This result also indicates that fetuses with isolated RAA-MB experience changes in vascular course but not in fetal hemodynamics.

Previous studies have indicated that infants with isolated RAA-MB generally have a more favorable prognosis (11,12). They typically do not exhibit clinical symptoms after birth, and only a small number require surgical intervention. Conversely, fetuses with RAA-MB and associated anomalies tend to have a relatively poorer prognosis due to the presence of additional cardiac and extracardiac abnormalities. These infants often experience more clinical symptoms after birth and typically require surgical treatment. Research indicates that due to prenatal vascular rings causing compression on the trachea and esophagus, the majority of infants will exhibit respiratory system symptoms postnatally (13,14). Respiratory symptoms may include wheezing, choking, episodes, and recurrent respiratory tract infections. Esophageal compression can cause swallowing difficulties, such as vomiting or food intolerance (15). In our study, the earliest onset of symptoms occurred more than 20 days after birth, with wheezing during crying being the primary manifestation. The maximum age at which symptoms appeared was 5 years. One patient experienced a sensation of choking while swallowing at the age of 4 years and underwent surgical treatment. By measuring changes in the fetal trachea, we can assess the degree of tracheal compression caused by the vascular ring and further predict the occurrence of respiratory symptoms after birth. Our study observed a direct correlation between the diameter of the main trachea at the level of the AO, the area within the vascular ring, and the symptoms experienced by the infants after birth. In the correlation analysis of 92 cases of VRA and TA in the patient group, the correlation coefficient was found to be 0.71. Our research results indicate that demonstrated a positive correlation between VRA and the symptoms experienced by fetuses after birth, indicating a direct relationship (16). VRA can serve as an indicator of the degree of tracheal compression to some extent. The smaller the vascular ring area during fetal development is, the more significant the compression on the trachea and esophagus, leading to the earlier onset of symptoms in fetuses after birth (17). Therefore, measuring the diameter of the main trachea at the level of the AO and the area within the vascular ring can provide a quantitative assessment of the prognosis of fetuses with vascular rings during prenatal evaluation. For fetuses with smaller VRA and TA measurements on prenatal ultrasound, close monitoring of the trachea for further tightening should be conducted after birth. The greater the difference in TA measurements is compared to normal fetuses, the earlier the onset and the more pronounced the symptoms of tracheal compression (18). Furthermore, our results indicated that some fetuses with RAA-MB had chromosomal abnormalities, and those with combined chromosomal abnormalities were more likely to experience tracheal compression symptoms after birth, suggesting a potential correlation between tracheal

cartilage compression and chromosomal abnormalities (19). Therefore, we recommend that fetuses prenatally diagnosed with RAA-MB and associated anomalies undergo additional chromosomal testing to rule out the possibility of chromosomal abnormalities.

We conducted follow-up observations on all patients included in the study. The findings revealed that two RAA-MB groups exhibited different clinical symptoms after birth. The RAA-MB with associated anomalies group displayed more severe clinical symptoms compared to the pure RAA-MB group, and the mortality rate was higher and the survival was lower in the RAA-MB with associated anomalies group. Moreover, the majority of those with RAA-MB and associated anomalies required surgical intervention after birth, which can be attributed to the complexity of concurrent intra- and extracardiac anomalies. We observed that patients with smaller ultrasound measurement parameters, including for TA, VRA, and AO-DA distance, were more likely to experience clinical symptoms and had a poorer prognosis after birth. Through univariate logistic regression analysis, we identified significant differences in TA, VRA, AO-DA angle, and AO-DA distance between the pure RAA-MB group and the RAA-MB group with associated anomalies. Building upon these analysis results, we further conducted multivariate logistic regression analysis and selected three ultrasound parameters, namely TA, VRA, and AO-DA distance, to develop a column chart prediction model for the prognosis of infants with RAA-MB. The model demonstrated AUC values of 0.799, 0.743, and 0.634 for TA, VRA, and AO-DA distance, respectively. Furthermore, the calibration curve closely aligned with the diagonal line, indicating the model's robust predictive performance and its ability to provide accurate prognosis for infants diagnosed prenatally with RAA-MB.

Most studies on this subject have primarily focused on the qualitative diagnosis of RAA-MB, with limited research on the quantitative analysis of adverse prognostic factors in infants with RAA-MB. The integration of prenatal ultrasound through combining qualitative diagnosis and quantitative analysis is crucial for evaluating the prognosis of infants with RAA-MB. In this study, we introduced a concise and clear column chart model that further enhances the assessment of combined ultrasound parameters in predicting the prognosis of infants with RAA-MB. The model demonstrated effective prognostic prediction, with a combined ROC curve area of 0.891 (95% CI: 0.789–0.914). These findings indicate that the constructed column chart model performs well overall,

and the clinical decision curve highlights its significant clinical benefits and high model value.

In light of these promising findings, some limitations should also be noted. First, the retrospective design and measurement of stored image data in this study introduced the potential risk of selection bias. Second, the sample size of infants with RAA-MB and associated anomalies was small. Therefore, it is necessary to conduct multicenter, prospective studies to further validate the effectiveness of the model and to evaluate its applicability in clinical practice.

Acknowledgments

Footnote

Reporting Checklist: The authors have completed the STROBE reporting checklist. Available at https://qims. amegroups.com/article/view/10.21037/qims-23-1648/rc

Conflicts of Interest: All authors have completed the ICMJE uniform disclosure form (available at https://qims. amegroups.com/article/view/10.21037/qims-23-1648/coif). The authors have no conflicts of interest to declare.

Ethical Statement: The authors are accountable for all aspects of the work in ensuring that questions related to the accuracy or integrity of any part of the work are appropriately investigated and resolved. This study was conducted in accordance with the Declaration of Helsinki (as revised in 2013) and was approved by the Ethics Committee of Gansu Provincial Maternity and Child-care Hospital. The participants provided their written informed consent to publish their cases (including publication of images).

References

1. Miranda JO, Callaghan N, Miller O, Simpson J, Sharland G. Right aortic arch diagnosed antenatally: associations and outcome in 98 fetuses. Heart 2014;100:54-9.
2. Zhang X, Zhu M, Dong SZ. Utility of fetal cardiovascular magnetic resonance imaging in assessing the fetuses with complete vascular ring. Front Pediatr 2023;11:1159130.
3. Zhang MX, Zhao BW, Pan M, Wang B, Peng XH, Chen R. Fetal Right Aortic Arch: A Quantitative Method of Outcome Prediction. Fetal Pediatr Pathol 2019;38:195-205.
4. François K, Panzer J, De Groote K, Vandekerckhove K, De Wolf D, De Wilde H, Marchau F, De Caluwe W, Benatar A, Bové T. Early and late outcomes after surgical management of congenital vascular rings. Eur J Pediatr 2017;176:371-7.
5. Cavoretto PI, Sotiriadis A, Girardelli S, Spinillo S, Candiani M, Amodeo S, Farina A, Fesslova V. Postnatal Outcome and Associated Anomalies of Prenatally Diagnosed Right Aortic Arch with Concomitant Right Ductal Arch: A Systematic Review and Meta-Analysis. Diagnostics (Basel) 2020;10:831.
6. Petrescu AM, Ruican D, Pătru CL, Zorilă GL, Tudorache Ş, Comănescu AC, Istrate-Ofiţeru AM, Badiu AM, Ioana M, Stoica GA, Iliescu DG. Prenatal findings and pregnancy outcome in fetuses with right and double aortic arch. A 10-year experience at a tertiary center. Rom J Morphol Embryol 2020;61:1173-84.
7. Biermann D, Holst T, Hüners I, Rickers C, Kehl T, Rüffer A, Sachweh JS, Hazekamp MG. Right aortic arch forming a true vascular ring: a clinical review. Eur J Cardiothorac Surg 2021;60:1014-21.
8. Galindo A, Nieto O, Nieto MT, Rodríguez-Martín MO, Herraiz I, Escribano D, Granados MA. Prenatal diagnosis of right aortic arch: associated findings, pregnancy outcome, and clinical significance of vascular rings. Prenat Diagn 2009;29:975-81.
9. Razon Y, Berant M, Fogelman R, Amir G, Birk E. Prenatal diagnosis and outcome of right aortic arch without significant intracardiac anomaly. J Am Soc Echocardiogr 2014;27:1352-8.
10. D'Antonio F, Khalil A, Zidere V, Carvalho JS. Fetuses with right aortic arch: a multicenter cohort study and meta-analysis. Ultrasound Obstet Gynecol 2016;47:423-32.
11. Vigneswaran TV, Allan L, Charakida M, Durward A, Simpson JM, Nicolaides KH, Zidere V. Prenatal diagnosis and clinical implications of an apparently isolated right aortic arch. Prenat Diagn 2018;38:1055-61.
12. Yan Y, Yang Z, Li Y, Pei Q, Zhang X, Wang Y, Yin X, Zhang L, Ren M, Liu G. The prenatal diagnosis and prognosis of fetal right aortic arch and double aortic arch malformation: A single-center study. J Obstet Gynaecol Res 2023;49:2273-82.
13. Gao J, Zhu J, Pei Q, Li J. Prenatal ultrasonic diagnosis and differential diagnosis of isolated right aortic arch with mirror-image branching. Arch Gynecol Obstet 2017;295:1291-5.
14. Velipasaoglu M, Sentürk M, Ayaz R, Atesli B, Tanir HM. Characteristics of prenatally detected right aortic arch cases in a single institution. J Obstet Gynaecol 2018;38:895-8.
15. Dong SZ, Zhu M. Prenatal cardiac magnetic resonance imaging of right aortic arch with mirror image branching and retroesophageal left ductus arteriosus. J Matern Fetal Neonatal Med 2019;32:1057-62.
16. Achiron RR, Kassif E, Gilboa Y, Salem Y, Jakobson Y, Raviv-Zilka L, Kivilevitch Z. Congenital Aortic Vascular Ring: In-Utero Sonographic Assessment of Tracheal Patency and Postnatal Outcome. Ultraschall Med 2022;43:e112-7.
17. Chiappa E, Ridolfi C, Cordisco A. The multiform sonographic spectrum of arterial duct in right aortic arch. Int J Cardiovasc Imaging 2021;37:3385-95.
18. Bartsota M, Jowett V, Manuel D, Mortensen K, Wolfenden J, Marek J, Carvalho JS. Double aortic arch: implications of antenatal diagnosis, differential growth of arches during pregnancy, associated abnormalities and postnatal outcome. Ultrasound Obstet Gynecol 2023;62:69-74.
19. Ismat FA, Weinberg PM, Rychik J, Karl TR, Fogel MA. Right aortic arch and coarctation: a rare association. Congenit Heart Dis 2006;1:217-23.